COMPARATIVE STUDY OF FRAMES USING VISCOELASTIC AND VISCOUS DAMPERS

By Yaomin Fu[1] and Kazuhiko Kasai,[2] Member, ASCE

ABSTRACT: Identical mathematical expressions for viscoelastic and viscous damper-brace components are derived as the function of two fundamental nondimensional parameters. These two parameters are used to investigate the properties of viscoelastic (VE) and viscous (VS) systems by conducting parameter analysis. Usually both VS and VE damper-brace components provide added stiffness and damping to the whole system. The magnitude of the added stiffness and damping depends not only on the damper, but also on the interaction of the damper with other members of the frame. Under conditions of low frequency and stiff brace, the added stiffness provided by a VS damper-brace component is negligible. Based on harmonic theory, closed-form solutions for seismic response prediction are presented and are used to determine the optimal design. As an example, the seismic performance of a 10-story steel frame incorporated with VE and VS dampers is studied.

INTRODUCTION

Among the many kinds of energy dissipators, viscoelastic (VE) and viscous (VS) dampers can be classified as one group, because they dissipate energy depending on the relative velocity between two ends of the damper. VE dampers (such as polymer dampers) usually provide resistance force with both in-phase and out-of-phase components. The properties of viscoelastic materials are usually frequency and temperature dependent (Kasai et al. 1993; Lai et al. 1996). VS dampers (such as fluid cylinders) can be designed to provide a purely viscous force. This means the damper-resistance force is out-of-phase with the damper deformation (Constantinou and Symans 1992; Taylor 1996). Although the damper fluid material may be temperature sensitive, such sensitivity can be reduced to achieve stable damper behavior. When installing VE or VS dampers into a frame, certain braces (or support members) are usually required. In this paper, the damper-brace component is referred to as the added component. The added component generally provides resistance forces both in-phase and out-of-phase with deformation, whether the damper force is purely VS or not. This phenomenon provides the basis to unify the mathematical descriptions of VE and VS systems and makes the two systems comparable.

This paper addresses the unified descriptions of VE and VS systems and focuses on comparative performances of these two systems. The similarities and differences in VE and VS system behavior are discussed. It is well known that the transient response component of a highly damped system decays very quickly and, therefore, the peak magnitude of the system's response is mainly governed by the harmonic response component. Based on this, the harmonic theory is used to derive various closed form solutions for VE or VS systems. These solutions are used to develop a response prediction method that establishes the relationship between the responses of the original system and the damped systems, using the two fundamental parameters that specify the added component. Thus, these fundamental parameters can be adjusted to achieve optimal design without dynamic analysis of the damped system. As an example, VE and VS dampers are used to retrofit a 10-story steel frame and analysis is conducted to show the comparative seismic performances and the validity of the prediction method.

[1]Visiting Res., Dept. of Civ. Engrg., Univ. of British Columbia, Vancouver, Canada.

[2]Prof., Struct. Engrg. Res. Ctr., Tokyo Inst. of Technol., Nagatsuta, Midori-Ku, Yokohama, Japan; formerly at ATLSS Center, Lehigh Univ., Bethlehem, PA 18015.

Note. Associate Editor: Chia-Ming Uang. Discussion open until October 1, 1998. To extend the closing date one month, a written request must be filed with the ASCE Manager of Journals. The manuscript for this paper was submitted for review and possible publication on April 7, 1997. This paper is part of the ***Journal of Structural Engineering***, Vol. 124, No. 5, May, 1998. ©ASCE, ISSN 0733-9445/98/0005-0513–0522/ $8.00 + $.50 per page. Paper No. 15552.

VE AND VS SINGLE-DEGREE-OF-FREEDOM (SDOF) SYSTEM CHARACTERISTICS

Constitutional Rule

The VE and VS dampers studied in this paper are assumed to be linear, and their constitutional force-deformation relationship can be expressed as follows (Kasai et al. 1993; Constantinou et al. 1993):

$$F_d(t) + aD^\alpha F_d(t) = k[u_d(t) + bD^\alpha u_d(t)],$$

$$D^\alpha = \frac{1}{\Gamma(1-\alpha)} \frac{d}{dt} \int_0^t \frac{d\zeta}{(t-\zeta)^\alpha} \quad \text{(VE damper)} \tag{1a}$$

$$F_d(t) = C_d \frac{du_d(t)}{dt} \quad \text{(VS damper)} \tag{1b}$$

where $F_d(t)$, $u_d(t)$ are the resistance force and deformation of the dampers respectively; a, b, k, and α are four constants specifying the viscoelastic damper; D^α is a fractional derivative operation; Γ is the gamma function; and C_d is the damping constant of the VS damper.

Harmonic Movement

In the frequency domain, assuming $u_d(t) = u_{d,\max} \sin \omega t$, the above equations become:

$$F_d(t) = K'_d u_{d,\max} \sin \omega t + K''_d u_{d,\max} \cos \omega t \quad \text{(VE damper)} \tag{2a}$$

$$F_d(t) = C_d \omega u_{d,\max} \cos \omega t \quad \text{(VS damper)} \tag{2b}$$

where K'_d and K''_d are storage stiffness and loss stiffness for the VE damper (Kasai et al. 1993).

$$K'_d = k \frac{1 + ab\omega^{2\alpha} + (a+b)\omega^\alpha \cos(\alpha\pi/2)}{1 + a^2\omega^{2\alpha} + 2a\omega^\alpha \cos(\alpha\pi/2)} \tag{3a}$$

$$K''_d = k \frac{(-a+b)\omega^\alpha \sin(\alpha\pi/2)}{1 + a^2\omega^{2\alpha} + 2a\omega^\alpha \cos(\alpha\pi/2)} \tag{3b}$$

In (2*a*) and (2*b*) the term involving sin ωt is the elastic force, and that involving cos ωt is the VS force. They are in-phase and 90° out-of-phase with deformation, respectively. Thus, (2*a* and *b*) can be rewritten as a single equation

$$F_d(t) = K'_d u_d(t) + K''_d u_d \left(t + \frac{\pi}{2\omega}\right) \tag{4}$$

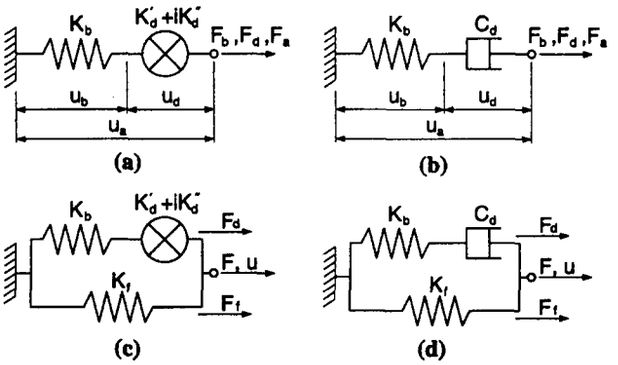

FIG. 1. VE and VS Mathematical Model: (a) VE Added Component; (b) VS Added Component; (c) VE System; (d) VS System

where $K'_d = 0$; and $K''_d = C_d\omega$ for the VS damper. It is noteworthy that the VS damper equations can be included in that of the VE damper. For the VE damper, K''_d increases with frequency up to a certain value (Lai et al. 1996), and obviously for the VS damper K''_d proportionally varies with frequency.

Added Component

Figs. 1(a and b) give mathematical models of added components for VE and VS systems, respectively, where K_b is the stiffness of the brace (or support member) used to install the damper in the frame structure; $K'_d + iK''_d$ represents the VE damper's ability to generate both elastic force and VS force coincident with its deformation; and $u_b(t)$ and $u_a(t)$ are the deformations of the brace and added component, respectively. According to the condition of compatibility and equilibrium

$$u_b(t) + u_d(t) = u_a(t) = u_{a,\max} \sin \omega t \tag{5a}$$

$$F_b(t) = F_d(t) = F_a(t) = K'_a u_{a,\max} \sin \omega t + K''_a u_{a,\max} \cos \omega t \tag{5b}$$

The last expression of (5*b*) assumes the general solution for resistance force of the added component discussed in frequency domain. By manipulating (4) and (5) and using $F_b(t) = K_b u_b(t)$, one can obtain the storage stiffness K'_a and loss stiffness K''_a of the added component

$$K'_a = \frac{(K_b + K'_d)K_b K'_d + K_b K''^2_d}{(K_b + K'_d)^2 + K''^2_d} \tag{6a}$$

$$K''_a = \frac{K_b^2 K''_d}{(K_b + K'_d)^2 + K''^2_d} \quad \text{(VE system)} \tag{6b}$$

$$K'_a = \frac{K_b K''^2_d}{K_b^2 + K''^2_d}; \quad K''_a = \frac{K_b^2 K''_d}{K_b^2 + K''^2_d} \quad \text{(VS system)} \tag{6c,d}$$

It is noteworthy that whether the damper has storage stiffness (VE damper) or not (VS damper), the added component always has both storage stiffness and loss stiffness and, therefore, provides both in-phase and out-of-phase resistance forces.

Frame Segment

The above simplified models [Figs. 1(c) and (d)] can be used to represent a frame segment shown in Fig. 2 in order to study the basic properties of the VE and/or VS systems. All quantities in Figs. 1 and 2 are measured in the lateral direction. K_f stands for the frame's shear stiffness. By assuming the system's deformation $u(t) = u_{\max} \sin \omega t$ and neglecting the damping effect of the original system, one can obtain the system's resistance force $F(t)$ [Figs. 1(c) and (d)]

$$F(t) = F_f(t) + F_a(t) = (K_f + K'_a)u_{\max} \sin \omega t + K''_a u_{\max} \cos \omega t \tag{7}$$

where K'_a and K''_a are calculated by (6); and $F_f(t) = K_f u_{\max} \sin \omega t$ is the resistance force provided by the frame. As before, the term involving sin ωt in (7) indicates the elastic force of the whole system [i.e., in-phase with the system's displacement $u(t)$]. Thus, the whole system's stiffness becomes $K_f + K'_a$, where K'_a is named as added stiffness. The term involving cos ωt in (7) indicates the viscous force of the whole system [i.e., out-of-phase with the system's displacement $u(t)$]. It is proportional to K''_a. Thus, K''_a reflects the added energy dissipation capability of the system. By interpolating $u(t) = u_{\max}$ sin ωt into (7), the force-displacement relationship [$F(t) - u(t)$] of the whole system can be obtained, as shown in Fig. 3. During one harmonic movement cycle, the maximum strain energy $E_s = (K_f + K'_a)u^2_{\max}/2$ and dissipated energy $E_d = \pi K''_a u^2_{\max}$.

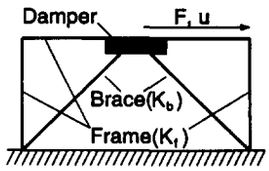

FIG. 2. Frame Segment

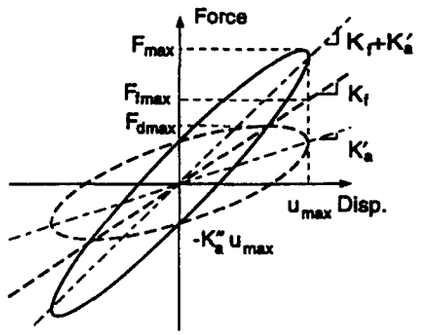

FIG. 3. Force-Displacement Relationship of VE or VS System

Nondimensional Parameters

When the excitation frequency ω reaches the system's resonance frequency (assuming a mass is attached to the right end of the system shown in Figs. 1(c) and (d)), the added damping ratio caused by damper $\xi_a = E_d/(4\pi E_s) = K''_a/[2(K_f + K'_a)]$ (Clough and Penzien 1992). By defining the added stiffness ratio $\alpha_a = K'_a/K_f$, (7) can be rewritten as follows:

$$F(t) = u_{\max} K_f (1 + \alpha_a)[\sin \omega t + 2\xi_a \cos \omega t] \tag{8a}$$

$$\alpha_a = \alpha_b \alpha''_d \frac{\alpha_b \eta_d + (1 + \eta_d^2)\alpha''_d}{(\alpha_b \eta_d + \alpha''_d)^2 + \eta_d^2 \alpha''^2_d}$$

$$\xi_a = \frac{1}{2} \frac{\alpha_b^2 \eta_d^2 \alpha''_d}{(\alpha_b \eta_d + \alpha''_d)(\alpha_b \eta_d + \alpha_b \alpha''_d + \alpha''_d) + (1 + \alpha_b)\eta_d^2 \alpha''^2_d} \text{ (VE)} \tag{8b,c}$$

$$\alpha_a = \frac{\alpha_b \alpha''^2_d}{\alpha_b^2 + \alpha''^2_d}; \quad \xi_a = \frac{\alpha_b^2 \alpha''_d}{2[\alpha_b^2 + (1 + \alpha_b)\alpha''^2_d]} \text{ (VS)} \tag{8d,e}$$

where $\eta_d = K''_d/K'_d$, the loss factor of the VE damper, is somewhat insensitive to the frequency and can be treated as a constant to simplify the analysis; $\alpha_b = K_b/K_f$ is the brace stiffness ratio; and $\alpha''_d = K''_d/K_f$ is the damper loss stiffness ratio, representing the energy dissipation capability of VE or VS damper. Eq. (8*d,e*) can be alternatively derived from (8*b,c*) by setting $\eta_d \to \infty$, because $K'_d = 0$ for a VS damper. For the VE damper case, the similar expressions were previously derived by using a so-called complex stiffness method (Kasai et al. 1994).

Parameter Analysis

The behavior of the damped system depends on both added stiffness ratio α_a and added damping ratio ξ_a. Furthermore, it can be seen from (8*b*–*e*), α_a and ξ_a are functions of α_b (brace stiffness ratio) and α_d'' (damper loss stiffness ratio), which are the fundamental parameters of the damped system.

Figs. 4(a and b) show added stiffness ratio α_a versus brace stiffness ratio α_b and damper loss stiffness ratio α_d'' for VE and VS systems, respectively. For both systems, increasing α_d'' causes increasing α_a. When α_d'' tends to infinity, α_a monotonously tends to its maximum value α_b. This tendency can be identified by (8*b*) and (8*d*) for VE and VS systems, respectively. This phenomenon is understandable because when the damper loss stiffness becomes very large, the damper tends to lock and only the brace deforms. This means either VE or VS damper-brace components can create added stiffness, which can be as large as brace stiffness, adding to the original system, especially under high mode motion, because both VE and VS dampers show rigid behavior under high frequency vibration. As α_d'' increases, the VE system's α_a approaches its maximum value α_b faster than the VS system, especially when the brace stiffness is large. Another tendency shown in Figs. 4(a and b) and revealed by (8*b*) and (8*d*) is that for a given α_d'', when α_b tends to infinity, α_a tends to $\alpha_d''/\eta_d = K_d'/K_f$ for VE systems, and zero for VS systems. Therefore, a stiff brace can increase the added stiffness for VE systems and eliminate added stiffness for VS systems. Fig. 4(a) also shows that for a VE system the maximum value of α_a is approximately α_d''/η_d for a given α_d'' when $\alpha_b \to \infty$. From (8*d*), the maximum value of α_a for a VS system is $\alpha_d''/2$ for a given α_d'', when $\alpha_b = \alpha_d''$. Thus, for the same parameter values, a VE system appears to have larger added stiffness than a VS system, and Fig. 4(b) shows that the latter appears to have negligible added stiffness in the conventional range if a stiff brace is used.

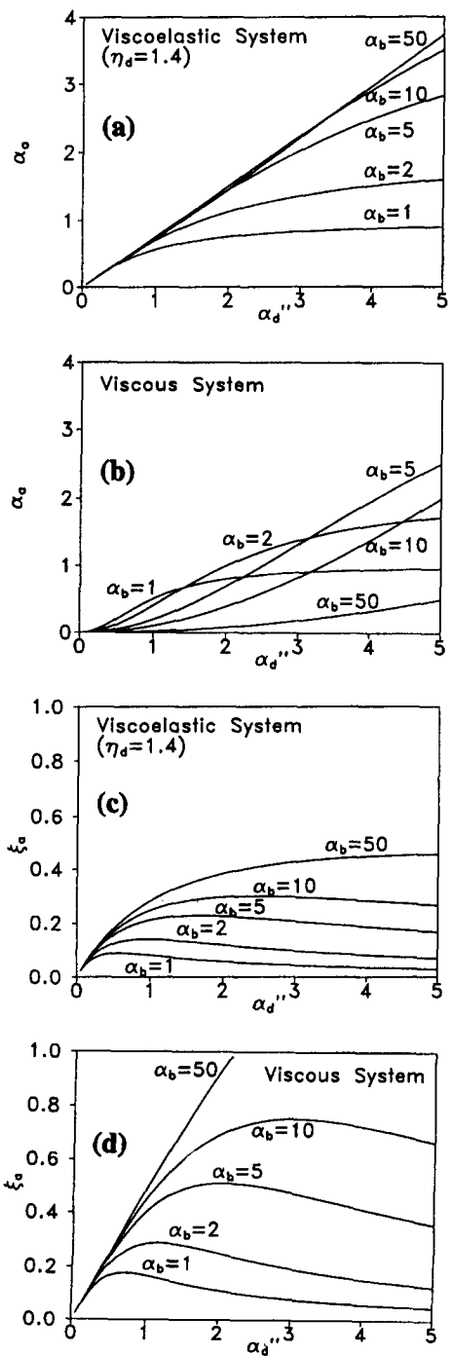

FIG. 4. Added Stiffness and Added Damping Ratio versus Brace Stiffness Ratio and Damper Loss Stiffness Ratio: (a) Added Stiffness Ratio of VE System; (b) Added Stiffness Ratio of VS System; (c) Added Damping Ratio of VE System; (d) Added Damping Ratio of VS System

Figs. 4(c and d) show the added damping ratio ξ_a versus brace stiffness ratio α_b and damper loss stiffness ratio α_d'' for VE and VS systems, respectively. The plots of ξ_a have similar aspects. A stiff brace (large α_b) always helps increase ξ_a. This phenomenon is also mentioned by Sause et al. (1994) in their similar nondimensional parameter analysis of the VE damped system. When a rigid brace is used ($\alpha_b = \infty$), for a given α_d'', ξ_a reaches maximum values of $\alpha_d''/2/(1 + \alpha_d''/\eta_d)$ for a VE system and $\alpha_d''/2$ for a VS system [Figs. 4(c and d)]. Therefore, VS systems can have much larger ξ_a than VE systems. For any given brace stiffness, there is a peak ξ_a [Figs. 4(c and d)] with respect to α_d''. Through manipulating (8*c*) and (8*d*) the peak damping ratio $\xi_{a,\text{peak}}$ can be derived for VE and VS systems, respectively:

$$\xi_{a,\text{peak}} = \frac{1}{4}\frac{\alpha_b\eta_d}{\sqrt{(1+\alpha_b)(1+\eta_d^2)} + 1 + \alpha_b/2},$$

$$\text{when } \alpha_d'' = \frac{\alpha_b\eta_d}{\sqrt{(1+\alpha_b)(1+\eta_d^2)}} \quad \text{(VE system)} \tag{9a}$$

$$\xi_{a,\text{peak}} = \frac{\alpha_b}{4\sqrt{1+\alpha_b}},$$

$$\text{when } \alpha_d'' = \frac{\alpha_b}{\sqrt{1+\alpha_b}} \quad \text{(VS system)} \tag{9b}$$

Comparing these equations and using a typical η_d value of about 1–1.4, this also suggests that, with the same brace stiffness, VS systems can have much larger ξ_a than VE systems. VE systems have lower ξ_a values because, with more stiffness gain, VE systems store more strain energy than VS systems, but dissipate almost the same amount of energy as VS systems, if the loss stiffness and the displacement for both systems is same.

HARMONIC RESPONSES

S_a–S_d Relationship

Using (8*a*), and including the original system's damping ratio ξ_o ($\xi = \xi_o + \xi_a$), the peak magnitude of the harmonic force ($F_{\max}$) of the entire system is

$$F_{\max} = u_{\max}K_f(1 + \alpha_a)\sqrt{1 + 4\xi^2} \tag{10}$$

Considering a mass M attached at right end of the system shown in Figs. 1(c and d) and assuming the system is excited by harmonic ground motion, at the steady state the peak

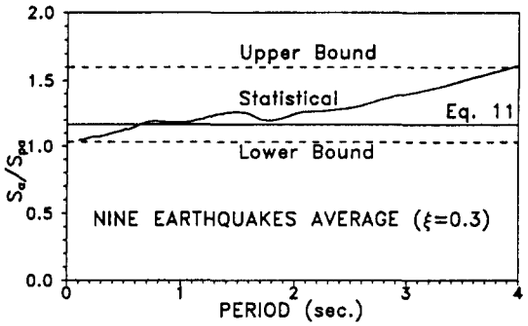

FIG. 5. Comparison of S_a/S_{pa} Calculation

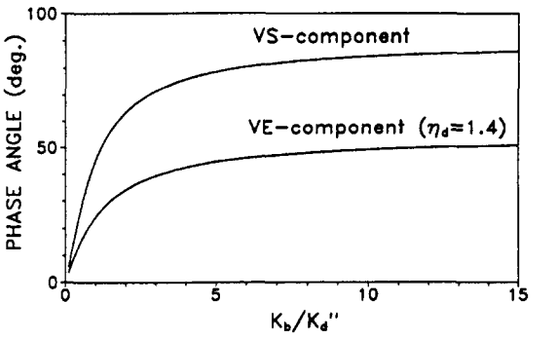

FIG. 6. Phase Angle between Force and Displacement of Added Component

system force $F_{max} = MS_a$, where S_a is the spectral acceleration due to the harmonic ground motion. Likewise, the peak steady state displacement $u_{max} = S_d$, where S_d is spectral displacement. The relationship between S_a and S_d can be derived from (10) as follows:

$$S_a(\xi, \omega) = \sqrt{1 + 4\xi^2}\omega^2 S_d(\xi, \omega) = \sqrt{1 + 4\xi^2} S_{pa}(\xi, \omega) \quad (11)$$

where $\omega = [K_f(1 + \alpha_a)/M]^{1/2}$ is the damped system's natural frequency and S_{pa} $(=\omega^2 S_d)$ is the so-called pseudoacceleration. It is well known (Clough and Penzien 1993) that S_a is not equal to S_{pa}, especially when ξ is larger than 10%. Eq. (11) gives an accurate relationship between S_a and S_{pa} only for steady-state harmonic movement. For random movement, if the harmonic response is predominant, it gives an approximate average measurement for the actual S_a–S_{pa} relationship, which has strong stochastic characteristics.

To show the validity of (11), a limited statistical analysis was conducted. Results are shown in Fig. 5 for $\xi = 30\%$. The analysis used eight recorded earthquakes (El Centro, Parkfield, Taft, Hachinohe, Sylmar, Pacoima, Mexico, and Newhall) and one artificial earthquake, whose 5% damping S_{pa} curve fits NEHRP (1991) seismic response coefficient with $Av = Aa = 0.4$ and $S = 1.2$ (see Fig. 12). Fig. 5 shows that the S_a/S_{pa} ratio calculated using (11) is close to the statistical result for periods of 0.5–2.5 sec. For periods of less than 0.5 sec, (11) overestimates the S_a/S_{pa} ratio. In the short period region, the ground motion is like step excitation rather than harmonic for a rigid system. As the period tends to zero, S_{pa} tends to S_a due to the solidity of the system. For periods larger than 2.5 sec, (11) underestimates the S_a/S_{pa}. In the long period region, the ground motion is like impulse excitation for a flexible system. As the period tends to infinity, S_{pa} tends to zero, and the S_a/S_{pa} ratio tends to infinity. An earlier study by Ashour et al. (1986) predicted that, in most cases, the S_a/S_{pa} ratio has a upper bound of $1 + 2\xi$ and lower bound of $(1 + 8\xi^4)^{1/2}$. These bounds are also shown in Fig. 5 for comparison.

Phase Angle

From (5*b*), the damper force (or added component force) is

$$F_d(t) = \sqrt{K_a'^2 + K_a''^2}\, u_{a,max} \sin(\omega t + \theta_a); \quad \tan\theta_a = K_a''/K_a' \quad (12a,b)$$

where θ_a is the phase angle between the damper force and the displacement of the damper-brace component. By substituting (6) into the above equation

$$\theta_a = \tan^{-1} \frac{\eta_d^2}{\eta_d + (1 + \eta_d^2)K_d''/K_b} \quad \text{(VE system)} \quad (13a)$$

$$\theta_a = \tan^{-1} \frac{K_b}{K_d''} \quad \text{(VS system)} \quad (13b)$$

When a rigid brace is used ($K_b/K_d'' \to \infty$), θ_a tends to 90° for VS-added components, indicating the resistance force is 90° out-of-phase with the displacement of the component. For VE-added components, θ_a is limited by $\tan^{-1}\eta_d$. The typical value of $\eta_d = 1-1.4$ for polymeric VE material leads to a maximum $\theta_a = 45°$ to 54°. Fig. 6 shows θ_a as a function of K_b/K_d'', and indicates that θ_a becomes insensitive when $K_b/K_d'' > 3$. For ensuring force-displacement out-of-phase characteristics in VS-added components, $K_b/K_d'' > 5$ is expected. However, for high mode motion, because K_d'' $(=\omega C_d)$ becomes large, it would be difficult to achieve $K_b/K_d'' > 5$ by using a reasonable amount of material for bracing.

Damper Force

Eq. (12) gives the peak damper force $F_{d,max}$

$$F_{d,max} = u_{max}\sqrt{K_a'^2 + K_a''^2} \quad (14)$$

By normalizing to the peak system force F_{max} (8*a*), the damper force ratio $F_{d,max}/F_{max}$ is

$$\frac{F_{d,max}}{F_{max}} = \sqrt{1 - \frac{1 + 2\alpha_a}{(1 + \alpha_a)^2(1 + 4\xi^2)}} \quad (15)$$

For frames, F_{max} is the peak story shear force and $F_{d,max}$ is the peak damper force measured in the lateral direction. The previous equation provides a method for estimating $F_{d,max}$ by scaling F_{max}.

Damper Deformation

When the added component deforms harmonically with a peak $u_{a,max}$ the damper deformation is (5)

$$u_d(t) = u_a(t) - \frac{F_a(t)}{K_b}$$

$$= u_{a,max} \sin\omega t - \frac{u_{a,max}}{K_b}(K_a' \sin\omega t + K_a'' \cos\omega t) \quad (16)$$

Thus, the peak damper deformation ($u_{d,max}$) can be measured by a given peak deformation of the added component ($u_{a,max}$)

$$\frac{u_{d,max}}{u_{a,max}} = \frac{K_b}{K_b + K_d'} \frac{1}{\sqrt{1 + [K_d''/(K_b + K_d')]^2}}$$

$$= \frac{1}{\sqrt{(1 + K_d''/K_b/\eta_d)^2 + (K_d''/K_b)^2}} \quad \text{(VE system)} \quad (17a)$$

$$\frac{u_{d,max}}{u_{a,max}} = \frac{1}{\sqrt{1 + (K_d''/K_b)^2}} \quad \text{(VS system)} \quad (17b)$$

The second expression in (17*a*) shows that the VE damper deforms less than a pure spring having stiffness K_d' when this spring connects in series with a brace having stiffness K_b. The $u_{d,max}/u_{a,max}$ ratio varies with respect to K_b/K_d'' as shown in Fig. 7. For VE-added component, the maximum damper deforma-

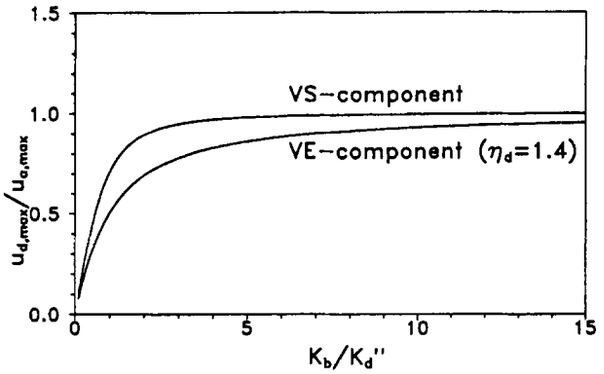

FIG. 7. Damper Deformation versus Added Component Deformation

tion is 86% of the total deformation of the added component when $K_b/K_d'' = 5$. In contrast, VS dampers show a larger deformation percentage, suggesting higher efficiency in energy dissipation. Eq. (17) can also be used to estimate the damper deformation demand for design purpose.

RESPONSE REDUCTION CAUSED BY ADDED STIFFNESS AND DAMPING

Spectrum Variation

By providing added stiffness and damping, supplemental dampers change the original system's period and damping ratio, and therefore influence the seismic response of the system. NEHRP (1991) assumes that the seismic coefficient, which is understood as pseudoacceleration S_{pa}, is inversely proportional to two-third power of the system's period if the period is not very small. Thus, due to period shifting, S_{pa} variation is

$$\frac{S_{pa}(T)}{S_{pa}(T_0)} = \left(\frac{T_0}{T}\right)^{2/3} \tag{18}$$

where T_0 and T are the periods of the original and damped systems, respectively. The response variation due to changing damping ratio from ξ_0 to ξ is represented by a simplified expression (Kasai and Fu 1995), which is very close to the NEHRP (1994) suggested value

$$D_\xi = \frac{S_d(\xi)}{S_d(\xi_0)} = \frac{\sqrt{1 + 25\xi_0}}{\sqrt{1 + 25\xi}} \tag{19}$$

Because the above equation appears to be close to the upper bound equation given by Hanson and Jeong (1994), it conservatively expresses the effect of damping on spectrum reduction.

Spectrum Response Reduction

Based on the above description, the spectral displacement reduction ratio R_{sd}, caused by added stiffness and damping, can be derived as:

$$R_{sd} = \frac{S_d(\xi, T)}{S_d(\xi_0, T_0)} = D_\xi \left(\frac{T}{T_0}\right)^{4/3} = \sqrt{\frac{1 + 25\xi_0}{1 + 25\xi}} (1 + \alpha_a)^{-2/3} \tag{20a}$$

Note that $1 + \alpha_a = (K_f + K_a)/K_f$ is a stiffness ratio that is proportional to $(T_0/T)^2$. Likewise, and using (11), the spectral acceleration reduction (variation) ratio R_{sa} can be derived as

$$R_{sa} = \frac{S_a(\xi, T)}{S_a(\xi_0, T_0)} = D_\xi \frac{\sqrt{1 + 4\xi^2}}{\sqrt{1 + 4\xi_0^2}} \left(\frac{T}{T_0}\right)^{-2/3}$$

$$= \sqrt{\frac{(1 + 25\xi_0)(1 + 4\xi^2)}{(1 + 25\xi)(1 + 4\xi_0^2)}} (1 + \alpha_a)^{1/3} \tag{20b}$$

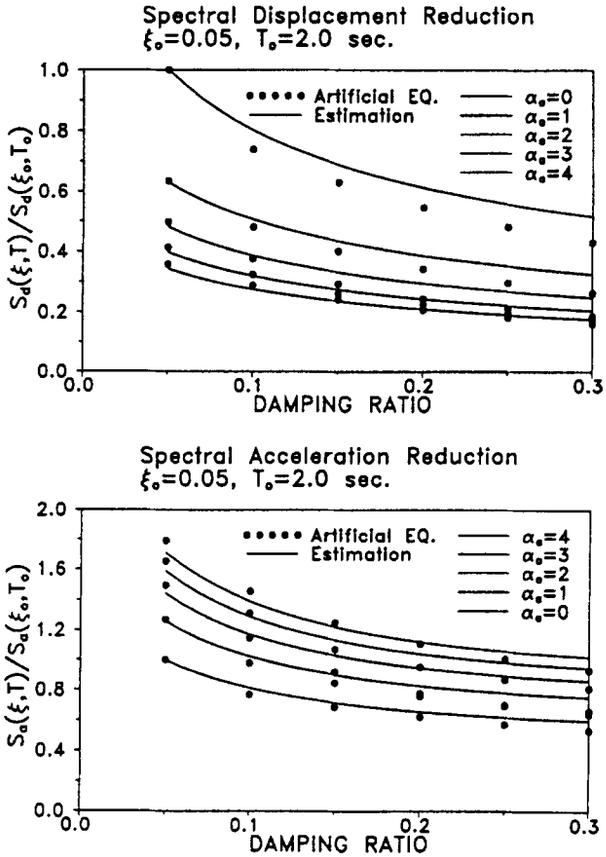

FIG. 8. Comparison of Spectrum Response Reduction Calculation

For comparison, R_{sd} and R_{sa} versus α_a and ξ are shown in Fig. 8, either estimated by (20) or calculated by time history integration of the aforementioned artificial earthquake record. Globally, (20) estimates fit the numerical results well, in spite of some conservatism due to the conservatism of the damping reduction rule (19). It is worthy to note that (20*a*) and (20*b*) are the combination of individual rules of NEHRP period shift (18), damping reduction (19), and S_a/S_{pa} ratio (11). Thus, their feasibility is determined by those rules, and their improvement depends on the appropriate selection of the individual rules. In addition, the fluctuation in actual earthquake response spectrum influences the response reductions predicted by (20). Kasai et al. (1998) have shown that the above methodology is reasonably accurate in predicting the average of the peak responses of the system under different earthquakes.

Response Prediction

By using (8*b*–*e*) and $\xi = \xi_o + \xi_a$, (20*a*) and (*b*) can be further expressed as the functions of α_d'' and α_b, which are the basic parameters of the damped system. For each pair of α_d'' and α_b, there is a corresponding pair of ratios R_{ad} and R_{sa}. Fig. 9 shows the relationships among R_{sd}, R_{sa}, α_d'', and α_b for VE and VS systems, respectively. It appears that a stiff brace has a positive effect in reducing either S_d and S_a responses. However, it is not necessary to use a rigid brace. $\alpha_b = 10$ or at least $\alpha_b > 5$ is recommended, because when $\alpha_b > 10$ the improvement in reduction is not significant, and for a VS system may even become worse. By increasing α_d'', S_d decreases if a relatively stiff brace is used ($\alpha_b > 5$). On the other hand, by increasing α_d'', S_a reduces at the beginning but increases after a turning point ($\alpha_d'' = 0.5$–1.0). Both S_d and S_a change significantly with respect to α_d'' before the returning point, but slowly beyond it, indicating the α_d'' insensitive region. Thus, $\alpha_d'' = 1$–1.5 is suggested for the best results. When the same

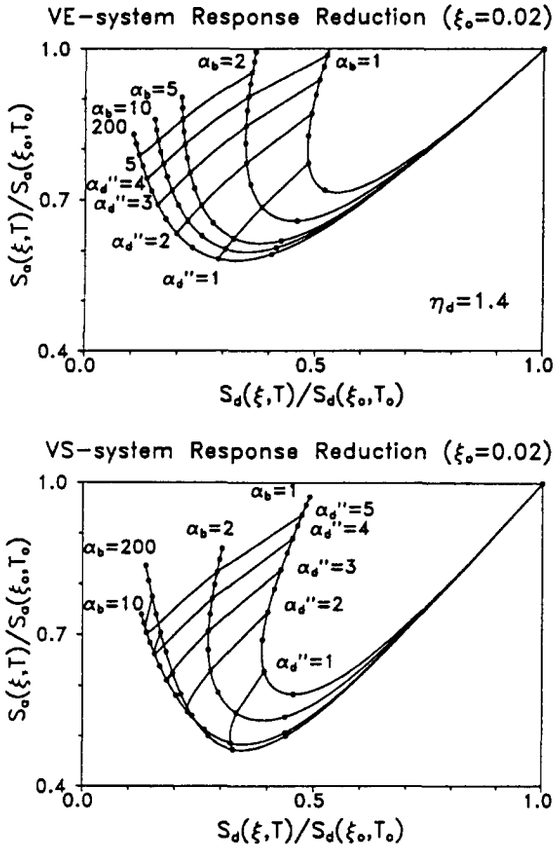

FIG. 9. Spectrum Response Reduction versus Brace Stiffness Ratio and Damper Loss Stiffness Ratio

parameters are selected, VE and VS systems have similar S_d reductions whereas VS systems have more S_a reduction. Fig. 9 also indicates that it is possible to achieve a minimum R_{sd} of 0.1 in either system, a minimum R_{sa} of 0.58 in a VE system with η_d = 1.4, and a minimum R_{sa} of 0.47 in a VS system.

Frame Response

The above discussion of response reduction in SDOF system can be illustrated by considering the retrofit of a moment resistant frame (MRF) using damper-brace components. In this case, the MRF is the original system, whereas the retrofitted frame is the damped system. Fig. 10 shows the harmonic force relationships in typical story segments of MRF and damped frames, where H = story height; and L = frame span length. For simplicity, the inflection point is assumed at the mid-height of the column. V_a and M_s are story shear force and over turning moment (OTM), respectively. V_a, V_c, and P_c are damper shear force, column shear force (per column), and column axial force, respectively. A subscript "o" is used to denote forces associated with the original MRF. Corresponding to SDOF system [Figs. 1(c and d)], the counterparts of F, F_f, and F_d are V_s, $2V_c$, and V_a, respectively. When subjected to harmonic movement, the story displacement is assumed to consist only of the sin ωt term, and the corresponding member forces are shown in Fig. 10 by considering their in-phase and out-of-phase characteristics. The superscript ′ denotes forces in-phase with displacement (sin ωt term) and ″ denotes forces out-of-phase with displacement (cos ωt term). In a MRF, all forces are assumed to be in-phase with the displacement by neglecting the small original frame damping. In a damped frame, M_s should have the same phase as V_s (i.e., $M_s'/M_s'' = V_s'/V_s''$), because both are caused by the same lateral load. The peak value of forces appearing in Fig. 10 (denoted by subscript

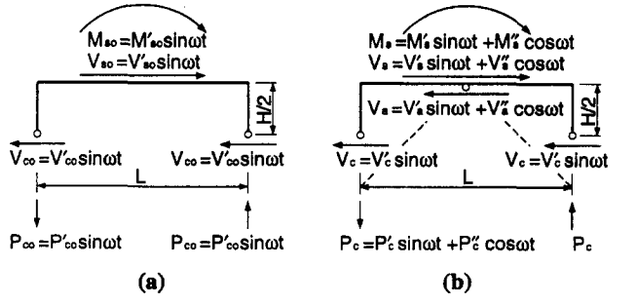

FIG. 10. Force Relationship in Frame Segment: (a) Original MRF; (b) Damped Frame

"max") are the square roots of the summation of the squares of the forces with superscripts ′ and ″.

Because S_d governs the frame's deformation, the reduction ratios of peak story displacement and peak story drift angle follow R_{sd} (20*a*). Because S_a is related to the inertial force, which is the lateral seismic load acting on the frame, the reduction ratios of peak story shear force ($V_{a,\max}/V_{so,\max}$) and peak story OTM ($M_{s,\max}M_{so,\max}$) follow R_{sa} (20*b*). The beam moments, column moments, and column shear force developed in the frame are associated with the frame deformation. Thus, the reduction ratios of the peak magnitude of these quantities are also expected to follow R_{sd}. The reduction ratio of peak column axial force (R_{pc}) can be derived by taking the moment equilibrium of the MRF and damped frame segments shown in Fig. 10

$$P'_{co} = \frac{M'_{so}}{L} + \frac{H}{L}V'_{co};\quad P_{co,\max} = P'_{co} \quad \text{(original MRF)} \qquad (21a)$$

$$P'_c = \frac{M'_s}{L} + \frac{H}{L}V'_c;\quad P''_c = \frac{M''_s}{L};\ P_{c,\max} = \sqrt{P'^2_c + P''^2_c}$$

(damped frame) (21*b*)

$$R_{pc} = \frac{P_{c,\max}}{P_{co,\max}} = \frac{R_{sa}}{\rho + 1}\sqrt{\rho^2 + \frac{2\rho}{(1+4\xi^2)(1+\alpha_a)} + \frac{1}{(1+4\xi^2)(1+\alpha_a)^2}};$$

$$\rho = \frac{P'_{co}}{V'_{co}}\frac{L}{H} - 1 \qquad (21c)$$

Equations $V'_c/V'_{co} = R_{sd}$, $M_{s,\max} = (M'^2_s + M''^2_s)^{1/2}$, $M_{a,\max}/M'_{so} = R_{sa}$, $M'_s/M_{s,\max} = (1 + 4\xi^2)^{-1/2}$ [induced from (8*a*) and (10)], and (20) are used to derive (21*c*) Eq. (21*c*) indicates that the column axial force reduction is not only related to α_a and ξ, but is also influenced by the peak column axial force $P_{co,\max} = P'_{co}$, as well as the peak column shear force $V_{co,\max} = V'_{co}$ of the original MRF. Note that (21) is suitable only for a frame with a single bay, but the same treatment can be expanded to more complicated situations.

The peak damper force $V_{a,\max}$ can be predicted by scaling the peak story shear force of the original MRF $V_{so,\max}$ ($=V'_{so}$) by the following ratio

$$R_{fd} = \frac{V_{a,\max}}{V'_{so}} = R_{sa}\frac{V_{a,\max}}{V_{s,\max}} = R_{sa}\sqrt{1 - \frac{1+2\alpha_a}{(1+\alpha_a)^2(1+4\xi^2)}} \qquad (22)$$

Note that V'_{so} = the summation of the total peak column shear forces of the MRF, $V_{a,\max}/V'_{so} = R_{sa}$, and $V_{a,\max}/V_{s,\max} = F_{d,\max}/F_{\max}$ (15).

The above discussion indicates that the peak responses of the damped frame can be predicted by scaling the peak responses of the original MRF without dampers. All scale factors listed above depend on the key parameters α_b and α''_d of the

damper-brace component. For more complicated situation, such like dampers incorporated in multi-bays or multi-dampers having different properties at the same story level, (21) and (22) need to be modified using the theories discussed herein.

SEISMIC RESPONSES OF MULTI-STORY FRAMES

Ten-Story Steel Frame Example

The frame used for this study is the minimum weight design Anderson-Bertero steel frame (1969) as shown in Fig. 11. Because this frame is a weak, flexible MRF, it can be used to show the effectiveness of supplemental dampers. The three different damper-brace components (VE, VS-1, and VS-2 frame) used are listed in Table 1. For all designs, the size of the brace is determined by the adequate stiffness ratio $K_b/K_f = 10$. VE frame uses VE dampers with damper loss stiffness ratio $K_d''/K_f = 1.2$ to optimize reduction of both deformation and story shear. VS-1 frame uses viscous dampers with the same loss stiffness ratio as VE frame. VS-2 frame also uses viscous dampers, but $K_d''/K_f = 0.5$ to achieve the same added damping ratio as VE frame. Elastic time history integration analyses were conducted to obtain each frame's responses. The analytical VE element (Kasai et al. 1993) was used to simulate both the VE and VS dampers because, as mentioned before, the VE constitutional rule (1*a*) can also include the VS version (1*b*). The VE damper material is 3M ISD-110 (Lai et al. 1996). For the VE frame calculation the ambient temperature is set to 24°C and temperature rise in the damper is suppressed. A structural damping ratio of 0.02 for the original MRF is assumed.

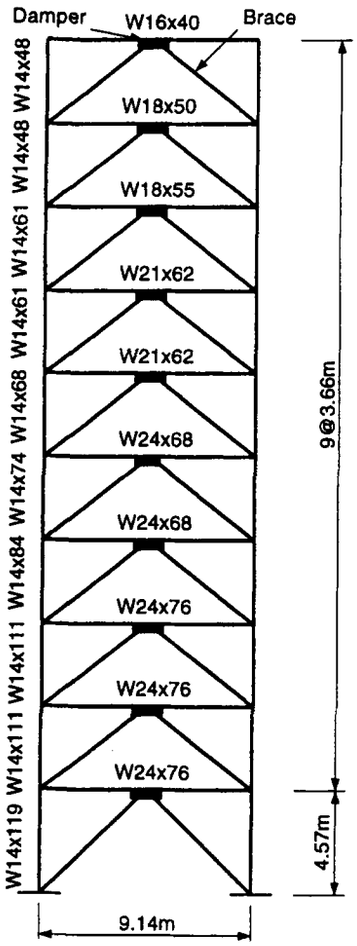

FIG. 11. Example Frame and Damper Location

By modifying the original modal strain energy method (Chang et al. 1992), the damping ratio of the retrofitted frame can be calculated as follows (Kasai and Fu 1995)

$$\xi_n = \frac{E_d}{4\pi E_s} = \frac{1}{2}\frac{\{\phi_n\}^T[K_a'']\{\phi_n\}}{\{\phi_n\}^T([K_f] + [K_a'])\{\phi_n\}} \tag{23}$$

where $\{\phi_n\}$ is the nth modal shape; $[K_f]$ is the stiffness matrix of the original frame; and $[K_a']$ and $[K_a'']$ are the matrix form of the storage and loss stiffness of the added component as calculated by (6). Note that because the high vibration mode of the damped frame is deeply suppressed with the supplemental damper, the damping ratio is calculated only for the first mode. From Table 1 it can be seen that with the same damper loss stiffness, the VS-1 frame can have much larger damping ratio and less period shifting than the VE frame.

Comparative Performance

The artificial earthquake record used earlier is adopted as excitation. The 5% damping S_{pa} curve of this artificial record simulates the NEHRP (1991) seismic response coefficient (Fig. 12). The first mode spectral response S_d and S_{pa} of the retrofitted frames and MRF are also shown in Fig. 12 for comparison.

Fig. 13(a) shows the peak responses of story shear force for MRF and damped frames. With supplemental dampers, the seismic loads are reduced to about one-half. Due to a shorter period (caused by larger stiffness) and a lower damping ratio, the VE frame has larger seismic loads than VS frames, with either equal loss stiffness or equal structural damping ratio. The two VS frames have nearly identical story shear forces, in spite of the significant difference in their damping ratios. Because the spectral acceleration S_a is related to story shear

TABLE 1. Structural Parameters for MRF and Retrofitted Frames

Story level (1)	M (kg) (2)	Brace K_b (kN/m) (3)	MRF K_f (kN/m) (4)	VE Frame K_d'' (kN/mm) (5)	VE Frame K_d' (kN/m) (6)	VS-1 Frame K_d'' (kN/m) (7)	VS-1 Frame C_d (kN-s/m) (8)	VS-2 Frame K_d'' (kN/m) (9)	VS-2 Frame C_d (kN-s/m) (10)
10	29,100	42,470	4,247	5,096	3,722	5,096	1,850	2,124	811
9	35,400	53,430	5,343	6,411	4,682	6,411	2,327	2,671	1,020
8	35,400	68,040	6,804	8,165	5,963	8,165	2,964	3,402	1,299
7	35,900	77,570	7,757	9,308	6,798	9,308	3,379	3,878	1,481
6	35,900	89,630	8,963	10,756	7,855	10,756	3,904	4,482	1,712
5	35,900	101,910	10,191	12,229	8,931	12,229	4,439	5,095	1,946
4	36,800	112,770	11,277	13,533	9,883	13,533	4,912	5,639	2,154
3	36,800	129,110	12,911	15,493	11,315	15,493	5,624	6,455	2,466
2	36,800	133,250	13,325	15,990	11,677	15,990	5,804	6,662	2,545
1	38,600	146,010	14,601	17,521	12,796	17,521	6,360	7,300	2,789

Note VE frame: $T = 1.80$ (sec), $\xi = 0.25$, $K_b/K_f = 10$, $K_d''/K_f = 1.2$, $\eta_d = 1.37$. VS-1 frame: $T = 2.28$ (sec), $\xi = 0.50$, $K_b/K_f = 10$, $K_d''/K_f = 1.2$. VS-2 frame: $T = 2.40$ (sec), $\xi = 0.25$, $K_b/K_f = 10$, $K_d''/K_f = 0.5$. MRF: $T_o = 2.43$ (sec), $\xi_o = 0.02$.

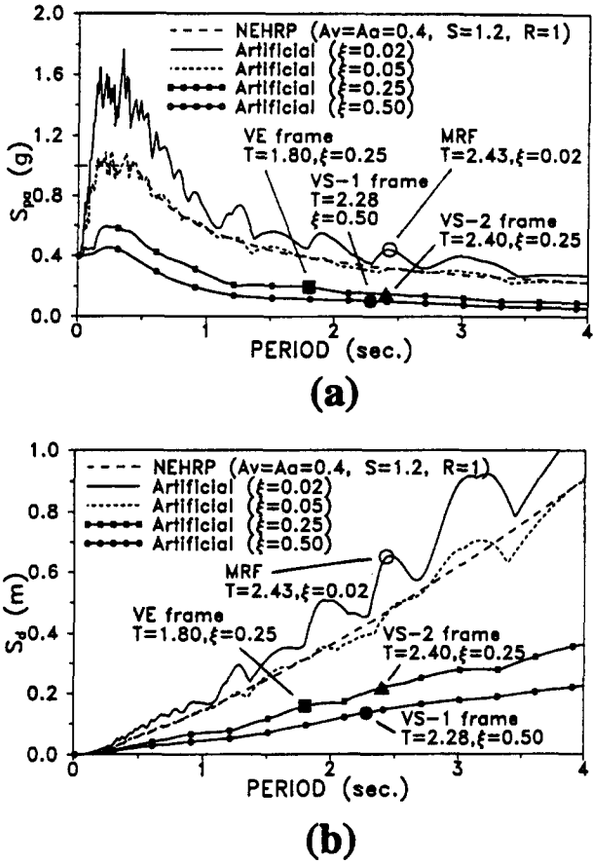

FIG. 12. NEHRP and Artificial Earthquake Spectrum: (a) Pseudoacceleration Spectrum; (b) Displacement Spectrum

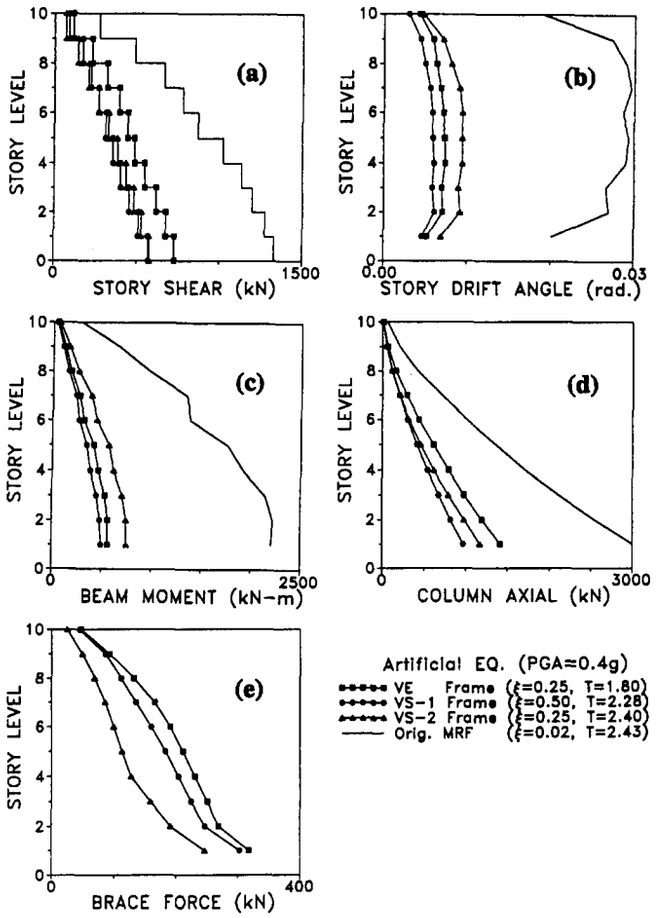

FIG. 13. Frame Responses; (a) Story Shear Force; (b) Story Drift Angle; (c) Beam Moment; (d) Column Axial Force; (e) Brace Force

force, Fig. 9 can be used to explain why the VE frame has larger shear forces and the two VS frames have similar shear forces. It is notable that Fig. 13(a) also reflects the tendency of OTM responses, because they are related to the lateral inertial load.

Fig. 13(b) shows the peak responses of story drift angle. It also shows that seismic deformation can be significantly reduced by the supplemental damper. By using the proposed optimal design, the drift can be controlled very well in both VE frame and VS frames. With the same damper loss stiffness, the VE frame has larger drift than the VS-1 frame due to less damping ratio, because the VE frame stores more strain energy, providing a larger denominator of (23). With the same damping ratio, the VE frame has smaller drift than the VS-2 frame, because the VE frame depends on both added stiffness and damping to suppress vibration, whereas the VS frame mainly depends on its damping effect. Fig. 12(b) also indicates this tendency.

Figs. 13(c–e) show the peak responses of the seismic member forces. Compared with the MRF, all VE and VS frames show significantly reduced member forces. It is known that beam moments accompany story drift. Hence the beam moments of damped frames have similar aspects to the story drifts of these frames. For the same reason, column shear forces and moments have a similar tendency as story drifts. Based on (21*b*), the column axial force is determined by story OTM and column shear force. Because of its larger story OTMs {evidenced by story shear forces [Fig. 13(a)]} and larger column shear forces {evidenced by story drifts [Fig. 13(b)}, the VE frame has larger column axial forces than the VS-1 frame. Compared to VS-2 frame, the VE frame still has larger column axial forces, even with smaller column shear forces {evidenced by story drifts [Fig. 13(b)]}. Because of larger K_a', the VE damper-brace components take more elastic story shear forces resulting in larger brace forces in the VE frame than in the VS frames. Similarly, comparing the two VS frames, the damper-brace component with larger K_a'' (VS-1 frame) produces more viscous force resulting in larger brace forces.

Fig. 14 shows the axial force (P_c)-moment (M_c) interactions of the 1st story columns for the four frames. In Fig. 14, the static force caused by gravity load are superimposed on the seismic results (P_c). It shows the dramatic improvement in the column strength demand due to the supplemental damper. Due to the larger seismic load [Fig. 13(a)], the VE frame's P_c–M_c curves slightly exceed the yield surface, whereas VS-1 frame's curves reach the surface. But having the same damping ratio as the VE frame, VS-2 frame's P_c–M_c curves exceed the yield surface due to the larger moment.

The M_c–P_c curves shown in Fig. 14 appear like inclined ellipse, which can be explained by using harmonic movement assumption (Fig. 10). Column axial force P_c has components both in-phase (P_c' sin ωt) and out-of-phase (P_c'' cos ωt) with the displacement (21*b*), whereas column moment M_c (=$0.5HV_c'$ sin ωt; Fig. 10) is in-phase with displacement. Thus, a time lag exists between M_c and P_c, resulting in an inclined elliptical P_c–M_c curve. Note that the P_c–M_c relationship is similar to $F(t)$–$u(t)$ relationship expressed by (7), shown in Fig. 3. The slope of the P_c–M_c ellipse is determined by the P_c'/V_c' ratio, whereas the fatness of the ellipse is determined by P_c''. By further deduction, it can be found that the ellipse slope is influenced by α_a, whereas the ellipse fatness depends on the frame's damping ratio ξ, which determines whether the seismic loads have the component out-of-phase with displacement (21*b*) and (8*a*). Evidenced by Fig. 14, the slope of the

P_c–M_c curve is not sensitive to α_a. Therefore, the frame's damping ratio is the main factor influencing the P_c–M_c curve. Although VE and VS added damper-brace components have different local effects on the original frame, their influence on the global damping ratio is similar (23). Accordingly the P_c–M_c curves in VE and VS frames become similar if these frames have same damping ratio. It would not be expected that the VS damper-brace component can cause P_c to increase out-of-phase with M_c without increasing the global damping, even though the component force has a 90° out-of-phase time lag (Fig. 6) with component deformation [Figs. 14(b) and (d)]. For earthquake response, the P_c–M_c ellipse will be deteriorated by the random behavior. In addition, the high mode effect can also cause the irregularity in the P_c–M_c curve, which has a strong appearance in the MRF's case [Fig. 14(a)].

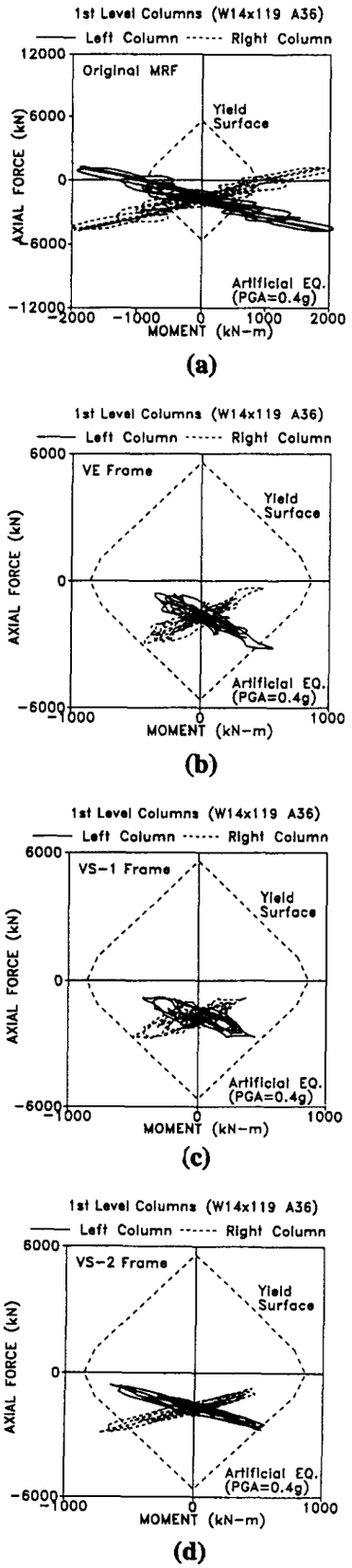

FIG. 14. Moment-Axial Force Interaction of First Floor Column: (a) MRF; (b) VE Frame; (c) VS-1 Frame; (d) VS-2 Frame

Response Reduction

To check the adequacy of (20)–(22) story response reductions were calculated using multi-earthquake analysis. Six earthquakes were used for the analysis Artificial (as before); El Centro; Parkfield; Hachinohe; Taft; and Sylmar. The reduction ratios were taken as the elastic responses of the VE frame or VS-1 frame over the elastic responses of the MRF. The average reduction ratios are shown in Figs. 15 and 16. Because the drift, displacement, beam moment, and column shear force are related to the deformation of the frame, the reductions in these quantities are compared with the spectral R_{sd} (Fig. 15). Because the story shear forces are related to acceleration, the reduction in story shear forces is compared with R_{sa} (Fig. 15). Also, the column axial force reduction and brace force scale factor are compared with the analytical expressions R_{pc} (21) and R_{fd} (22), respectively, as shown in Fig. 16. Corresponding to the added components parameters $\alpha_b = 10$ and $\alpha_d'' = 1.2$, the VE system has closed form solutions of $R_{sd} = 0.28$, $R_{sa} =$

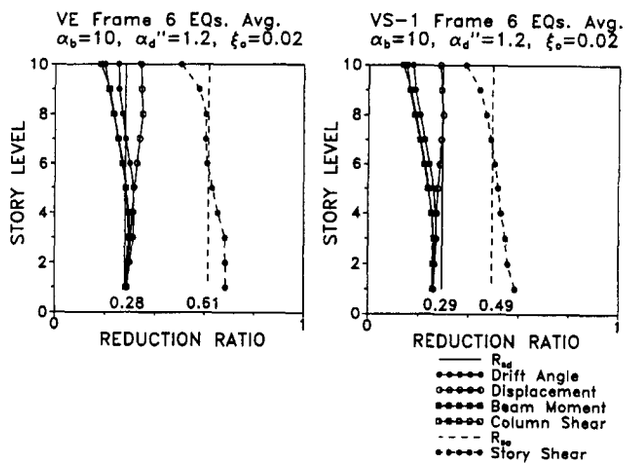

FIG. 15. Comparison of Response Reduction Predictions Related to S_d and S_a

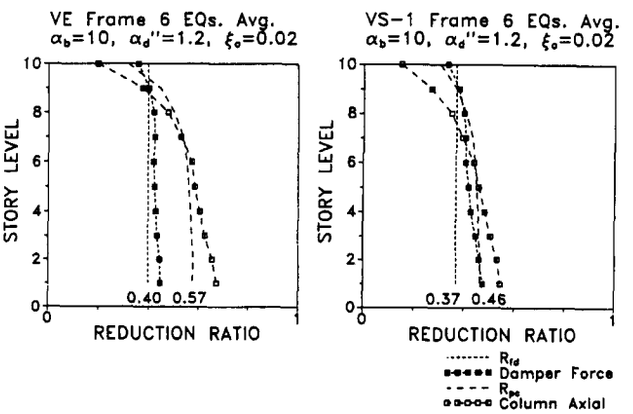

FIG. 16. Comparison of Response Reduction Predictions of Column Axial and Brace Force

0.61, R_{pc} = 0.57 (the first floor), and R_{fd} = 0.40, whereas the VS system has R_{sd} = 0.29, R_{sa} = 0.49, R_{pc} = 0.46 (the first floor), and R_{fd} = 0.37. These reductions are calculated for the frame's first mode, which predominately governs the frame responses. It is notable that for higher modes the response reductions differ according to the selected parameters of the added component. This causes additional errors when the closed form solutions are used to estimate the frame responses. However, the comparisons shown in Figs. 15 and 16 indicate that the SDOF estimates correlate well with the frame's statistical results.

CONCLUSION

Both VE and VS damper-brace components induce added stiffness and damping to the system. Conventionally, a system with supplemental VE damper gains both added stiffness and damping, whereas a system with VS damper primarily gains adding damping under conditions of low frequency movement. For harmonic excitation, damping effectively reduces the peak displacement response, and thus reduces elastic member force of the frame, such as beam and column moment. However, for impulse excitation, stiffness plays a more important role than damping in reducing the peak displacement response.

With adequate design (Fig. 9), the resistance force provided by a viscous damper-brace component can be 90° out-of-phase with the component's deformation. However, this does not necessarily cause the column axial force to increase 90° out-of-phase with the column moment. Rather, the global damping of the frame influences the interaction between column axial force and column moment. In the other words, VE- and VS-added components have the same effect on column axial force if they provide the same added damping ratio to the frame.

For energy dissipation, VS damped systems have slightly higher efficiency than VE systems, because VS dampers can deform more than VE dampers when the added component is subjected to the same deformation. The example designs show that with the same damper loss stiffness, the seismic performances of VS damped frames are slightly better than those of VE damped frame, whereas with the same damping ratio, the performances of VE frames are better. When using either type of damper, a significant reduction in frame seismic load and deformation can be expected.

To achieve the optimal results, the ratio of brace stiffness to frame stiffness (α_b) equal to 10, and the ratio of damper loss stiffness to frame stiffness (α''_d) equal to 1.0–1.5, are recommended for either VE- or VS-added components. The response prediction method presented in the paper works well in the range of structural period equal to 0.5–2.5 sec, and it can be further improved by improving the individual constitutional rules such as damping reduction, period shifting and relationship between spectral acceleration and displacement.

ACKNOWLEDGMENTS

The writers are grateful to Nippon Steel Corporation, National Science Foundation, and 3M Company, for their sponsorship to this research project. However, the opinions expressed do not necessarily reflect the views of the sponsors.

APPENDIX. REFERENCES

Anderson, J. C., and Bertero, V. V. (1969). "Seismic behavior of multistory frames designed by different philosophies." *EERC Rep. No. 69-11*, Earthquake Engrg. Res. Ctr., University of California at Berkeley, Calif., 35.

Ashour, A., Hanson, R. D., and Scholl, R. E. (1986). "Effect of supplemental damping on earthquake response." *Proc., ATC Seminar on Base Isolation and Passive Energy Dissipation*, Applied Technology Council, Redwood City, Calif., 271–280.

Chang, K. C., Soong, T. T., Oh, S.-T., and Lai, M. L. (1992). "Seismic response of steel-frame structures with added viscoelastic dampers." *Proc., 10th World Conf. on Earthquake Engrg.*, A. A. Balkema, Rotterdam, The Netherlands, Vol. 9, 5169–5173.

Clough, R. W., and Penzien, J. (1993). *Dynamics of structures*. McGraw-Hill, Inc., New York, N.Y., 56–58, 577.

Constantinou, M. C., and Symans, M. D. (1992). "Experimental and analysis investigation of seismic response of structures with supplemental fluid viscous dampers." *NCEER Rep. No. 92-0032*, Nat. Ctr. for Earthquake Engrg. Res., State University of New York at Buffalo, N.Y., 1–20.

Constantinou, M. C., Symans, M. D., Tsopelas, P., and Taylor, D. P. (1993). "Fluid viscous dampers in applications of seismic energy dissipation and seismic isolation." *Proc., ATC-17-1 Seminar on Seismic Isolation, Passive Energy Dissipation, and Active Control*, Applied Technology Council, San Francisco, Calif., 581–592.

Hanson, R. D., and Jeong, S.-M. (1994). "Design procedure utilizing supplemental energy dissipation devices for improved building performance." *Proc., 5th Nat. Conf. on Earthquake Engrg.*, Earthquake Engrg. Res. Inst., Chicago, Ill., 517–526.

Kasai, K., Munshi, J. A., Lai, M.-L., and Maison, B. F. (1993). "Viscoelastic damper hysteretic model: Theory, experiment, and application." *Proc., ATC-17-1 Seminar on Seismic Isolation, Passive Energy Dissipation, and Active Control*, Applied Technology Council, San Francisco, Calif., 521–532.

Kasai, K., Fu, Y., and Lai, M.-L. (1994). "Finding of temperature-insensitive viscoelastic frames." *Proc. 1st World Conf. on Struct. Control*. Int. Assn. for Struct. Control, Los Angeles, Calif., WP3-3.

Kasai, K., and Fu, Y. (1995). "Seismic analysis and design using viscoelastic dampers." *Proc., of Symp. on a New Direction in Seismic Design*, Architectural Inst. of Japan, Tokyo, Japan, 113–140.

Kasai, K., Fu, Y., and Watanabe, A. (1998). "Two types of passive control systems for seismic damage mitigation." *J. Struct. Engrg.*, ASCE 124(5), 501–512.

Lai, M. L., Lu, P., Lunsford, D. A., Kasai, K., and Chang, K. C. (1996). "Viscoelastic damper: a damper with linear or nonlinear material?" *Proc. 11th World Conf. on Earthquake Engrg.*, Elsevier Science Ltd., Acapulco, Mexico, No. 795.

NEHRP recommended provisions for seismic regulations for new buildings. (1991). *Part 1–Provisions*, Building Seismic Safety Council, Washington, D.C., 52.

NEHRP recommended provisions for seismic regulations for new buildings. (1994). *Part 1–Provisions*, Building Seismic Safety Council, Washington, D.C., 76.

Sause, R., Hamingway, G. J., and Kasai, K. (1994). "Simplified seismic response analysis of viscoelastic-damped frame structure." *Proc., 5th Nat. Conf. on Earthquake Engrg.*, Earthquake Engrg. Res. Inst., Chicago, Ill., 839–848.

Taylor, D. P. (1996). "Fluid damper for applications of seismic energy dissipation and seismic isolation." *Proc., 11th World Conf. on Earthquake Engrg.*, Elsevier Science Ltd., Acapulco, Mexico, No. 798.